Treatment of monogenic and digenic dominant genetic hearing loss by CRISPR-Cas9 ribonucleoprotein delivery *in vivo*

Veronica Lamas Alvarez
Department of Otology and Laryngology, Harvard Medical School
Yong Tao
Massachusetts Eye and Ear Infirmary
Yiran Li
Department of Otology and Laryngology, Harvard Medical School
Wan Du
Department of Otology and Laryngology, Harvard Medical School
Madelynn Whittaker
Gladstone Institutes https://orcid.org/0000-0002-3382-1134
John Zuris
Merkin Institute of Transformative Technologies in Healthcare, Broad Institute of MIT and Harvard
David Thompson
Harvard University
Wenliang Zhu
Department of Otology and Laryngology, Harvard Medical School
Arun Prabhu Rameshbabu
Department of Otology and Laryngology, Harvard Medical School https://orcid.org/0000-0001-8599-569X
Yilai Shu
ENT institute and Department of Otorhinolaryngology, Eye & ENT Hospital, State Key Laboratory of Medical Neurobiology and Institutes of Biomedical Sciences, Fudan University
Xue Gao
Rice University https://orcid.org/0000-0003-3213-9704
Johnny Hu
Merkin Institute of Transformative Technologies in Healthcare, Broad Institute of MIT and Harvard
Wei-Jia Kong
Huazhong University of Science and Technology https://orcid.org/0000-0001-5410-2297
Xueazhong Liu
Department of Otolaryngology, University of Miami Miller School of Medicine
Hao Wu

Shanghai Ninth People's Hospital
Benjamin Kleinstiver
Massachusetts General Hospital and Harvard Medical School https://orcid.org/0000-0002-5469-0655
David Liu
Broad Institute
Zheng-Yi Chen (Zheng-Yi_Chen@meei.harvard.edu)
Department of Otology and Laryngology, Harvard Medical School https://orcid.org/0000-0002-1452-4193

Article

Keywords:

Posted Date: July 15th, 2022

DOI: https://doi.org/10.21203/rs.3.rs-1836399/v1

Version of Record: A version of this preprint was published at Nature Communications on August 15th, 2023. See the published version at https://doi.org/10.1038/s41467-023-40476-7.

Abstract

Mutations in Atp2b2, an outer hair cell (OHC) gene, cause dominant hearing loss (HL) in humans. Using a mouse model Atp2b2Obl+, with a dominant HL mutation (Oblivion), we show that liposome-mediated in vivo delivery of CRISPR-Cas9 ribonucleoprotein (RNP) complexes leads to specific editing of the Obl allele. Large deletions encompassing the Obl locus and indels were identified as the result of editing. In vivo genome editing promotes OHC survival and restores OHC function, leading to robust hearing rescue. We further show in a double-dominant mutant mouse model, in which the Tmc1 Beethoven mutation and the Atp2b2 Oblivion mutation cause di-genic genetic HL, RNP delivery targeting both mutations lead to hearing rescue. These findings suggest that liposome-RNP delivery can be used as a strategy to rescue hearing with dominant mutations in OHC genes and with di-genic mutations in the auditory hair cells, expanding therapeutics of gene editing to treat HL.

Introduction

Deafness affects about 466 million people, including 34 million children, constituting 6% of the global population (http://www.who.int/en/). The most common type is sensorineural hearing loss (SNHL) whose pathogenesis occurs in the inner ear, the sensory organ or the auditory nerve. Hereditary types of hearing loss account for more than 50% of all congenital sensorineural hearing loss cases and are caused by genetic mutations *(1)*. To date, 119 genetic loci have been linked to hereditary hearing loss (http://hereditaryhearingloss.org/), but there are currently no biological treatments for any form of hereditary deafness *(2, 3)*. In the last two decades, the use of gene therapy strategies as treatment for inner ear dysfunction has emerged as a powerful therapeutic approach in deafness mice. Gene replacement using adeno-associated viral (AAV) vectors, gene silencing using either antisense oligonucleotides or AAV delivered microRNAs were strategies that have shown promising results in improving hearing in mouse models of deafness *(4–7)*. However, these approaches have limitations including the size of genes to be inserted into an AAV, inefficient targeting dominant mutations, and potential long term safety concerns of viral vectors.

The advent of genome editing has made possible to therapeutically intervene genetic diseases fundamentally at genomic DNA level. Furthermore, the recent discovery and development of CRISPR-associated protein 9 (Cas9)-based genome editing has facilitated the effective targeted gene disruption or repair of virtually any sequence of interest in the genome, and has been used to treat hereditary diseases in mouse models *(8–12)*. We and others have applied the CRISPR-based gene editing agents to rescue hearing in mouse models of human genetic deafness. By lipid and AAV mediated delivery of *Streptococcus pyogenes* Cas9 (SpCas9) ribonucleoprotein (RNP) complexes, we and others improved hearing in a mouse model of dominant hearing loss of hair cell origin, the Beethoven (*Bth*) mouse, by targeting the mutant allele of the transmembrane channel-like 1 (Tmc1) *(13, 14)*. Recently, the new generation of base editors were used to repair a recessive mutation on the *Tmc1* gene, which

transiently improved hearing in the Baringo mice *(15)*. The editing treatment for hearing loss, however, has been limited to inner hair cells (IHC) due to the primary role of *Tmc1.* Auditory function requires functional inner and outer hair cells (OHC). Further, multiple genetic hearing loss has been shown to be associated with mutations in OHC genes *(16)*. In our editing treatment of the Beethoven mutant mice for hearing rescue, we detected deterioration in OHC function shown by distortion product of acoustic emissions (DPOAE) in the treated inner ears *(13)*, raising the question if our liposome mediated delivery and editing is suitable to target OHC mutations to rescue hearing. Thus, it is necessary to address the limited efficiency of the gene editing therapies in targeting and functionally rescuing the OHC.

To evaluate liposome delivery of gene editing targeting the OHCs, we selected a dominant deafness mouse model (*Atp2b2*$^{Obl/+}$ mouse), which carries a mutation Oblivion (*Obl*) in the second isoform of the plasma membrane Ca^{2+}-ATPase (*Atp2b2*) gene that impairs the calcium pumping ability of the PMCA2 protein. The PMCA2 calcium pump is produced at high level in the stereocilia bundle of the OHC *(17)*. Mutations of PMCA2 Ca^{2+} pump of the stereocilia cause deafness and loss of balance in both mice and humans *(18–20)*. *Obl* heterozygous mice show progressive hearing loss starting at P20 and progressive degeneration of the sensory hair cells. *Obl* homozygous mutants are completely deaf from birth, and show a severe degeneration of the organ of Corti. In this work we apply our previously described CRISPR-Cas9 lipid-mediated delivery paradigm to the Oblivion mouse model to rescue hearing loss of the OHC origin. We first selected and evaluated the ability and specificity of different sgRNAs in disrupting the *Obl* mutation *in vitro*. Then, we performed lipid mediated delivery of Cas9 and sgRNA ribonucleoprotein complexes into the inner ear of postnatal heterozygous *Atp2b2*$^{Obl/+}$ mouse to rescue hearing loss.

Although most cases of genetic deafness result from mutations at a single locus, an increasing number of examples are being recognized in which mutations at two loci are involved. For example, digenic interactions are known to be an important cause of deafness in individuals who carry mutations at the Connexin 26 and 30 loci *(21)*, or Connexin 26 and 31 loci *(22)*. Pathogenic digenic inheritance has also been seen in Pendred *(23)* and Usher syndromes *(24)*, and an *Atp2b2* mutation was found in a deafness family with a homozygous *Cdh23* mutation *(18)*. For these cases, editing therapy that targets both mutations will be necessary for hearing rescue. Here, we performed editing to target two mutations simultaneously, the Oblivion mutation in the *Atp2b2* gene and the Beethoven mutation in the *Tmc1* gene, in a deaf mouse model that harbors both mutations, which led to hearing rescue. Our results strongly support the feasibility of liposome-mediated delivery of editing RNP to target dominant mutations of auditory hair cells in hearing rescue.

Results

Screening sgRNAs *in vitro*

To develop a genome-editing strategy capable of disrupting the mouse *Obl* mutant allele, we began by searching for protospacer sequences at the target site. We identified three sgRNAs that target *Atp2b2* at the sites that include the *Obl* (c.C2630T, p.S877F) mutation and a nearby NGG protospacer adjacent motif (PAM) sequence required by SpCas9. The three candidate sgRNAs (*Atp2b2*-mut1, *Atp2b2*-mut2, and *Atp2b2*-mut3) place the *Obl* mutation at the position of 18, 12, and 20, respectively, of the spacer, counting the PAM as positions 21-23 **(Fig. 1a)**. We evaluated the ability of these sgRNAs when complexed with Cas9 to cleave either the wildtype (WT) or the *Obl* allele *in vitro*. All three sgRNAs cleaved the *Obl* allele, with *Atp2b2*-mut1 exhibiting the greatest selectivity for the *Obl* over the wildtype *Atp2b2* gene **(Fig. 1b, c).** To evaluate the allele specificity of genomic modification in mouse cells, we treated adult mouse primary fibroblasts with Cas9:*Atp2b2*-mut1 by plasmid DNA nucleofection. After nucleofection, we measured the insertion and deletion mutation (indel) efficiency at the on-target by next-generation sequencing (NGS) and detected indels (0.6-2%) in both $Atp2b2^{Obl/+}$ and $Atp2b2^{Obl/Obl}$ mouse primary fibroblasts (**Fig. 1d, e)**. In contrast, no indels were detected in the wildtype (WT) control mouse primary fibroblasts (**Fig. 1d, e**). The common small DNA modifications were 1-2 bp deletions around the predicted Cas9 cleavage site (**Fig. 1e**).

The low indel rate (0.6-2%) may reflect low editing efficiency in the adult mouse primary fibroblasts. To improve the editing efficiency in order to better evaluate the specificity of genomic editing on the *Obl* allele, we generated a cell line, *Obl*-OC1, by inserting a mouse genomic DNA fragment harboring the *Obl* mutation into the WT mouse inner ear cell line, HEI-OC1 *(25)*. We isolated the genomic DNA from cells transfected with Cas9 protein complexed with each of the three sgRNAs by nucleofection and performed T7E1 assay and NGS analysis to evaluate cleavage and the indel frequency at the target sites (**Supplementary Fig. 1a, b**). The gRNAs *Atp2b2*-mut2 and *Atp2b2*-mut3 resulted in cleavage in WT and *Obl Atp2b2* DNA (**Supplementary Fig. 1a**) from the T7E1 assay. The gRNA *Atp2b2*-mut1 produced the cleavage products only in the *Obl*-OC1 cells **(Supplementary Fig. 1a)**, an indication of high selectivity at the *Obl* allele by *Atp2b2*-mut1 gRNA. NGS analysis showed a high rate of indels on the *Obl* allele in the *Obl*-OC1 cells with 34.8% from Cas9:*Atp2b2*-mut1, 79.5% from Cas9:*Atp2b2*-mut2, and 66.4% from Cas9:*Atp2b2*-mut3 treatment (**Supplementary Fig. 1b, c**). The indel analysis showed that Cas9:*Atp2b2*-mut1 exhibited the highest specificity on the *Obl* site with no detectable editing events in the WT *Atp2b2* locus from HEI-OC1 cells (**Supplementary Fig. 1b, c**). In contrast, *Atp2b2*-mut2 and *Atp2b2*-mut3 edited the WT HEI-OC1 cells. The results support that *Atp2b2*-mut1 mediated the most efficient discriminatory editing on the *Ob1* allele (**Fig. 1e**) and thus was selected in the *Obl* mouse model study.

Off-target analysis

The design of genome editing- based therapies requires the assessment of potential off-target effects to determine the specificity of editing, as the outcome of editing therapy relies on efficient on-target editing in order to be efficacious and the reduction in off-target effects to minimize potential safety concerns. As CRISPR-Cas agents may modify both on-target and off-target loci *(26, 27)*, we studied potential off-target loci that could be cleaved by Cas9:*Atp2b2*-mut1 by computational prediction *(28)* and the GUIDE-seq method *(26)*. Computational prediction identified five potential off-target sites (**Supplementary Fig. 2a**) containing up to three mismatches in the protospacer region of *Atp2b2*-mut1 sgRNA by computational prediction using the CRISPR Design Tool *(28)*. None of these loci are associated with hearing function (**Supplementary Fig. 2b**). We measured the indel frequency at each off-target site by NGS analysis in Cas9:*Atp2b2*-mut1 treated *Obl*-OC1 cells following nucleofection of RNP or plasmids DNA. Plasmid nucleofection resulted in 0.69% indels in the WT *Atp2b2* locus and 0.16% indels in Off-T4 site (**Supplementary Fig. 2c**). In contrast, RNP treatment exhibited no detectable editing events in either WT allele or other off-target sites (**Supplementary Fig. 2c**), consistent with the data (**Supplementary Fig. 1c**) and our previous findings that RNP delivery greatly reduces off-target sites *(8, 13)*. We further performed GUIDE-seq to unbiasedly analyze cleaved off-target loci in *Obl*-OC1 cells nucleofected with Cas9:*Atp2b2*-mut1 RNPs. Only the *Atp2b2* locus was identified by GUIDE-seq (**Supplementary Fig. 2d**). Consistent with NGS analysis of computationally predicted sites, no off-target loci were observed by GUIDE-seq method in *Obl*-OC1 cells nucleofected with RNP. As control we performed QUIDE-seq on the gene *Vbp1* after nucleofection with the Cas9:*Vbp1*-gRNA RNP in *Ob1-OC1* cells. QUIDE-seq analysis identified indels at multiple *Vbp1* off-target sites (**Supplementary Fig. 2e**). Together, these results support that delivery of Cas9:*Atp2b2*-mut1 RNP complexes into *Obl*-OC1 cells leads to no detectable off-target modification, and that any potential phenotype affecting hearing due to editing are unlikely to arise from off-target modifications.

In vivo editing with Cas9:*Atp2b2*-mut1 results in indels and large deletions

Efficient editing in hair cells *in vivo* is likely one of the most important factors determining the extent and duration of hearing rescue in the $Atp2b2^{Obl/+}$ mice. Hair cells constitute a small percentage of all cochlear cells, which makes it challenging to measure editing efficiency in hair cells when DNA from whole cochleae is used for analysis. In order to more precisely characterize editing at the *Obl* locus in hair cells *in vivo*, we injected Cas9-GFP:*Atp2b2*-mut1:lipo2000 into the inner ear of P1 $Atp2b2^{Obl/+}$ mice. Four days after injection, the organ of Corti was harvested with the GFP positive sensory epithelium dissected from the rest of the cochlea so the transfected sensory epithelium was enriched. Following DNA extraction and PCR amplification of the genomic region harboring the *Obl* and WT alleles, we performed NGS analysis to assess the editing efficiency. We observed an indel rate of 1% in the *Obl Atp2b2* locus in the injected $Atp2b2^{Obl/+}$ organ of Corti samples (**Fig. 2a**). No editing events were observed in the samples from uninjected contralateral control or WT $Atp2b2^{+/+}$ mice injected with Cas9-GFP:*Atp2b2*-mut1 (**Fig. 2a**).

The relatively low *in vivo* indel rate in the inner ear could result from inefficient editing *in vivo* and/or other chromosomal organizational changes including editing-induced large deletions which could not be detected by amplicon-based NGS analysis. If editing results in for instance large deletions harboring the mutant allele, our detection method to identify small indels could miss it. To assess if large deletions could be the result of editing undetected by NGS, we performed nested PCR on the DNA isolated from the RNP injected *Atp2b2*$^{Obl/+}$ inner ear *in vivo*, using two pairs of nested flanking primers that were more than 1 kb apart in the genomic DNA centered around the cutting site defined by the sgRNA, to amplify both large (without large deletions) and small (with large deletions) DNA fragments **(Fig. 2b**). Nested PCR yielded large and small DNA fragments in the editing complex injected samples (**Fig. 2c**). NGS study of these small fragments revealed multiple deletions of DNA fragments of ~1.7 kb that harbored the *Obl* mutation in exon 24, with the ends of the deletions in the intronic regions flanking exon 24 (**Fig. 2d**). The results demonstrated that Cas9-GFP:*Atp2b2*-mut1 *in vivo* injection caused large deletions encompassing the *Obl* mutation.

In the *Atp2b2*$^{Obl/+}$ inner ears, both WT and the *Obl* alleles were transcribed and translated specifically in the OHCs, with the protein products recognized by the antibody. We were thus unable to use immunolabeling to differentiate the *Atp2b2* from *Atp2b2*^{Obl} products as readout for editing event. As an alternative to study editing effect, we compared the ratio between WT and *Obl* alleles based on genomic DNA using purified hair cells. This comparison based on DNA is more sensitive than the comparison of WT and *Obl* transcripts as only two copies of DNA instead of multiple copies of mRNA present in each hair cell. We performed the study by harvesting and dissecting the cochleae from RNP injected and uninjected *Atp2b2*$^{Obl/+}$ inner ears, with the cochleae incubated with the vital dye FM1-43 to label hair cells. We then dissociated the cochleae so hair cells could be visualized and individually picked under an inverted fluorescent microscope for DNA extraction. We performed whole genome amplification on DNA from isolated hair cells followed by PCR and NGS to identify WT and *Obl* alleles. In uninjected *Atp2b2*$^{Obl/+}$ hair cells, we detected an *Obl*:WT ratio percentage of 52.57±3.47:47.5±3.48 (mean ± sd). In injected hair cells, an *Obl*:WT ratio percentage of 46.18±2.55: 53.25±2.27 (mean ± sd) was detected. There was 6.4% shift from the *Obl* towards the WT allele in hair cells after injection (**Fig. 2e**). As the *Atp2b2*-mut1 only targets the *Obl* allele (**Supplementary Fig. 2c**)*,* the data suggests that in as many as 25% of the HCs the *Obl* mutant allele was disrupted by editing, so the WT *Atp2b2* allele in the edited hair cells could restore HC function. Combining the indels, the large deletions and the change in the allele frequency in favor of WT *Atp2b2* gene, these results support that RNP delivery by Lipo2000:Cas9/sgRNA *Atp2b2*-mut1 into the inner ear of *Atp2b2*$^{Obl/+}$ mice *in vivo* result in conventional indels and uncommon large deletions around the cutting site, and as the result disrupt the *Obl* mutation in a significant number of hair cells.

In vivo editing on the *Obl* mutation of *Atp2b2* gene preserves outer hair cell morphology and survival

The *Atp2b2* gene is specifically expressed in

the cochlear outer hair cells (OHC) *(29)*. Previous studies have shown that the *Atp2b2*$^{Obl/+}$ mice exhibited progressive base to apex degeneration of hair cells, with OHC more affected than inner hair cells (IHC) *(20)*. To evaluate the effect of the Cas9:*Atp2b2*-mut1 sgRNA complex to target the *Obl* allele in the OHCs *in vivo*, we complexed the Cas9:*Atp2b2*-mut1 sgRNA with Lipofectamine 2000 and injected the mixture into the scala media of neonatal (P0-2) *Atp2b2*$^{Obl/+}$ mice by cochleostomy, with the mouse inner ears harvested at 2 months of age. We used an anti-Parvalbumin antibody to label all hair cells and an anti-PMCA2 antibody to visualize the distribution of PMCA2, the protein encoded by the *Atp2b2* gene, in the OHC. In uninjected *Atp2b2*$^{Obl/+}$ inner ear, there was a severe loss of HCs. In the high frequency region (45.25 kHz), virtually all OHCs (PMCA2^{+}) were absent with some missing IHC, whereas in other frequency regions, partial loss of OHCs was evident (**Fig. 3a, b**). In contrast, in the injected *Atp2b2*$^{Obl/+}$ ears, most of the OHCs survived in the cochlea across all frequency regions at this age (**Fig. 3a, b**). There is a generally greater IHC loss in uninjected inner ear although it is not statistically significant (**Fig. 3c**). Examination of stereocilia of the OHC and IHC revealed that after RNP delivery, the *Atp2b2*$^{Obl/+}$ hair cells had well preserved stereocilia morphology; whereas in uninjected *Atp2b2*$^{Obl/+}$ hair cells of the contralateral inner ear, the stereocilia morphology was disrupted (**Fig. 3d**). These results demonstrate that Cas9/*Atp2b2*-mut1/Lipo2000 injection *in vivo* rescues *Atp2b2*$^{Obl/+}$ hair cells by promoting OHC survival and maintaining the stereocilia structure in *Atp2b2*$^{Obl/+}$ mice.

In vivo editing on the *Obl* mutation of *Atp2b2* gene restores OHC function and rescues hearing

The goal of our study is to use editing to target the dominant OHC *Atp2b2 Obl* mutation to rescue hearing. PMCA2 plays an essential role in the OHC function by regulating the Ca^{2+} level to maintain homeostasis of the cochlea *(17)*. In the *Atp2b2*$^{Obl/+}$ mice the *Obl* mutation has dominant effect that disrupts the function of PMCA2 and consequently the OHC function measured by the elevated thresholds of the distortion product otoacoustic emissions (DPOAEs) *(20)*. The lack of OHC function results in profound hearing loss in the *Atp2b2*$^{Obl/+}$ mice *(20)*.

To evaluate the ability of the Cas9:*Atp2b2*-mut1 sgRNA complex to rescue OHC function, we injected lipid-mediated delivery of Cas9*:Atp2b2*-mut1 sgRNA complexes into neonatal (P0-P2) *Atp2b2*$^{Obl/+}$ mice and analyzed the DPOAEs from four weeks onwards. Wildtype one month old C3H mice, with the same genetic background as the *Atp2b2*$^{Obl/+}$, were included for the measurement as additional controls. Four weeks after injection, *Atp2b2*$^{Obl/+}$ untreated ears showed elevated DPOAEs thresholds ranging from 75-80 dB SPL across all frequencies, a demonstration of virtually complete lack of the OHC function (**Fig. 4a**). In contrast, in the injected *Atp2b2*$^{Obl/+}$ inner ears, DPOAE thresholds were significantly reduced in most frequencies of 8 to 45.24 kHz (**Fig. 4a**) with the thresholds of 45-75 dB SPL, representing reductions of 9-32 dB SPL depending on the frequency. Compared to the same age WT C3H mice, injected

Atp2b2$^{Obl/+}$ ears recovered an average 44% of DPOAE thresholds vs uninjected ears across the frequencies of 8 to 45.24 kHz. At 16 kHz in the injected ears, DPOAE recovered to 68% of that in WT C3H ears. The frequency 5.66 kHz did not show a significant threshold change among injected, uninjected *Atp2b2*$^{Obl/+}$ and C3H inner ears.

The lack of OHC function leads to profound hearing loss in the *Atp2b2*$^{Obl/+}$ mice. To study the effect of Cas9:*Atp2b2*-mut1 sgRNA injection on hearing in *Atp2b2*$^{Obl/+}$ mice, we measured auditory brainstem responses (ABRs), which assays the sound evoked neural output of the cochlea. Uninjected *Atp2b2*$^{Obl/+}$ inner ears showed elevations in cochlear neural responses at 4-week of age, with ABR thresholds ranging from 70-90 dB, compared with the 30-40 dB for wildtype C3H mice (**Fig. 4b**). In contrast, injected *Atp2b2*$^{Obl/+}$ ears showed significantly improved neural cochlear responses four weeks after injection, with lower ABR thresholds relative to uninjected ears (**Fig. 4b, c**). Significant hearing preservation was detected in all frequencies, with average ABR thresholds 26 dB lower in the treated ears than untreated contralateral ears. Compared with C3H control ears, injected *Atp2b2*$^{Obl/+}$ ears recovered hearing to 55% of the normal level. Greater wave I amplitudes were seen in the injected than uninjected ears (**Fig. 4d)**. A normal ABR waveform pattern was observed in the treated ears whereas in uninjected ears waveform pattern was absent (**Fig. 4e**).

As a behavioral measure of hearing preservation, we assessed acoustic startle responses eight weeks after injection. Uninjected *Atp2b2*$^{Obl/+}$ mice showed profound attenuation of startle responses following stimulus at 100, 110 and 120 dB SPL individually, with the amplitudes 0-4 mV rms, compared to the 10-25 mV rms in the wildtype C3H mice (**Fig. 4f**). In contrast, injected *Atp2b2*$^{Obl/+}$ mice showed significant ($P<0.001$) startle responses following stimulus at 110 and 120 dB SPL compared to the uninjected mice, with the startle response amplitudes that were similar or equal to those observed in the wild type C3H mice (**Fig. 4f**). Thus, RNP delivery of the editing complex restored startle responses in *Atp2b2*$^{Obl/+}$ mice as the result of hearing rescue.

Long term recovery of OHC function and hearing

We continued the test of DPOAE and ABR of injected ears at eight and 16 weeks after injection. We observed that the improvement in OHC activity achieved at four weeks was maintained in the treated ears at frequencies ranged from 11.32 to 22.64 kHz eight weeks after the injection, with average DPOAE thresholds 22 dB SPL lower for the treated ears than untreated contralateral ears (**Supplementary Fig. 3a**). Smaller but significant ($P < 0.01$) improvement in DPOAE thresholds was still detected at 11.32 and 16 kHz 16 weeks after injection (**Supplementary Fig. 3b**). Significant hearing rescue in the

Atp2b2$^{Obl/+}$ mice treated with Cas9/*Atp2b2*-mut1/Lipo2000 was maintained at eight and 16 weeks after injection. ABR threshold reductions were significant at the frequencies below 32 kHz at eight weeks with an average reduction of 20 dB (**Supplementary Fig. 3c**), and at the frequencies below 16 kHz at 16 weeks with an average reduction of 14 dB after the injection (**Supplementary Fig. 3d**).

Hearing rescue is gRNA specific and depends on the disruption of the *Obl* allele and the Cas9 cleavage activity

From the *in vitro* assay, the gRNA *Atp2b2*-mut1 showed the highest editing discriminating the *Obl* allele, thus was chosen for the *in vivo* study. Two other gRNAs, *Atp2b2*-mut2 and *Atp2b2*-mut3, were less specific as they targeted the *Obl* and the WT alleles (**Fig. 1b; Supplementary Fig. 1)**. To assess the ability of other less efficient *Atp2b2 Obl*-targeting sgRNAs in rescue of OHC function and hearing, we injected Cas9:*Atp2b2*-mut2:Lipo2000 complexes into P1 neonatal *Atp2b2*$^{Obl/+}$ mice. Four weeks after injection, we did not detect any improvement in the DPOAE or ABR thresholds of the *Atp2b2*$^{Obl/+}$ injected ears compared to the contralateral uninjected ears (**Supplementary Fig. 4a, b)**. Thus the *in vitro* selection of the gRNA with the highest specificity on the mutant *Obl* allele predicated the *in vivo* functional study outcome.

To test whether amelioration of hearing loss requires the disruption of the mutant *Atp2b2 Obl* allele, we injected Cas9/sgRNA/lipid complexes targeting an unrelated gene (GFP) in *Atp2b2*$^{Obl/+}$ mice and observed no significant improvements in ABR or DPOAE thresholds (**Supplementary Fig. 4c, d**). In addition, to test whether preservation of cochlear function requires Cas9 nuclease activity, rather than transcriptional interference from Cas9 binding to *Atp2b2*, we injected *Atp2b2*$^{Obl/+}$ mice with catalytically inactive dCas9 complexed with *Atp2b2*-mut1 sgRNA and observed lower but not statistically different ABR or DPOAE thresholds in injected and uninjected ears (**Supplementary Fig. 4e, f**). Taken together, these results support that the hearing rescue in *Atp2b2*$^{Obl/+}$ mice is *Obl* allele specific and depends on Cas9 DNA cleavage activity.

Double editing partially rescues hearing loss of digenic mutation origin *in vivo*

Increasingly, genetic hearing loss has been shown to be caused by digenic mutations, i.e. mutations in two different genes *(30, 31)*. Editing approach to rescue hearing would require editing that targets both mutations simultaneously. To establish the feasibility that RNP mediated delivery of editing agents can target two separate mutations from different genes simultaneously, we bred two dominant mouse models *Atp2b2*$^{Obl/+}$ with *Tmc1*$^{Bth/+}$ to create a digenic dominant hearing loss model *Atp2b2*$^{Obl/+}$;*Tmc1*$^{Bth/+}$(double mutant), in which the *Obl* mutation primarily affects the OHC

whereas the *Bth* affects the IHC. We performed liposome mediated delivery of Cas9 complexed with individual *Atp2b2*-mut1 sgRNA, *Tmc1*-mut3 sgRNA or the mixture of both into the scala media of neonatal (P1) double mutant mice and tested the hearing one month after the injection. We have previously demonstrated that Cas9:*Tmc1*-mut3 sgRNA:Lipo2000 injection rescued hearing in the $Tmc1^{Bth/+}$ model *(13)*. Uninjected double mutant ears exhibited severely damaged auditory function shown by large shifts in ABR and DPOAE thresholds across all frequencies (**Supplementary Fig. 5a, b**). In the double mutant inner ears injected with the mixture of Cas9:*Atp2b2*-mut1/ *Tmc1*-mut3 gRNAs, we detected significant hearing rescue for the frequencies below 22.64 kHz with an average reduction in the ABR thresholds of 14 dB (13.61±1.472, mean±s.d, n=9) (**Supplementary Fig. 5a**). Lower but not statistically significant DPOAE thresholds at 11.32 and 16 kHz were also detected in the injected inner ears (**Supplementary Fig. 5b**). Injections of Cas9 complexed with single gRNA targeting the *Obl* or the *Bth* mutation individually failed to rescue hearing (**Supplementary Fig. 5c-f**). Taking together these results suggest that rescue from hearing loss of digenic mutations requires two specific sgRNAs targeting the two mutations at the same time.

Discussion

PMCA2 is essential to OHC function and is required for hearing *(17–20)*. Outer hair cells are known to be the most vulnerable components of the auditory system and their malfunction is implicated in the sensory hearing loss pathologies. Without proper functional OHC, hearing sensitivity and frequency selectivity are impaired *(32)*. Despite the importance of the OHC in hearing, no previous therapeutic approaches have been developed to target and restore the function of the OHC for hearing restoration. Mutations in the *Atp2b2* have been associated with dominant progressive hearing loss in human *(19)*. An *Atp2b2* variant has also been shown to be a modifier that contributes to the severity of hearing loss *(18)*. In mice, the *Obl* mutation is shown disrupt the resting activity of the Ca^{2+} pump in the OHC that sets the peak Ca^{2+} level to the baseline in a semi-dominant manner that leads to progressive hearing loss *(20)*. Given the importance of PMCA2 in the OHC function and hearing loss, and the dominant transmission pattern, the *Obl* mouse model is a good model to study using editing to disrupt the mutation and to rescue hearing.

We have previously demonstrated the feasibility of liposomal mediated RNP delivery of editing agents in hearing rescue in a mouse model of human genetic hearing loss DFNA36 *(13)*. In that model however, the mutation Beethoven in the *Tmc1* gene primarily affects inner hair cells. Further DPOAE thresholds in the treated inner ears were elevated comparing to uninjected control ears. This raised a question if our approach is suitable to target OHC to edit mutations for hearing rescue.

The current work shows that liposome mediated delivery of Cas9-sgRNA RNP complexes in the inner ear leads to editing that abolishes the *Obl* mutation in the *Atp2b2* gene, restoring the functions of OHCs with improved cell survival and rescue of hearing in dominant genetic mouse model Oblivion with OHC deficit. The functional recovery quantified here using physiological and behavioral assays suggests that transient lipid-mediated delivery of RNP complexes may be a good therapeutic strategy to target OHC for editing, and rescue hearing of dominant genetic OHC dysfunction. Combined with our previous work on editing for hearing rescue in the inner hair cells *(13)*, it supports that liposomal mediated RNP delivery can be applied to rescue hearing in dominant hearing loss models of inner and/or outer hair cell origin.

Our study shows robust rescue in DPOAE and ABR thresholds after injection of editing agents in the *Atp2b2*$^{Obl/+}$ inner ear. This is likely due to efficient editing at the *Obl* allele. By NGS and indel analysis from the *Atp2b2*$^{Obl/+}$ adult primary fibroblasts treated by nucleofection of the RNP complex *in vitro* or from the *Atp2b2*$^{Obl/+}$ inner ears injected with the complex *in vivo,* the overall indel rate is relatively low (~1%), which suggested that the analysis underestimated the editing efficiency. A few factors may have contributed to the low indel rate detected. First, editing in the *Atp2b2* locus in adult fibroblasts may be intrinsically less efficient than in other rapidly dividing cell type. After we used the transposon to introduce the DNA fragment harboring the *Obl* mutation into an organ of Corti cell line that is rapidly dividing, we detected an indel rate of 40% after nucleofection of the same RNP complex, suggesting cell type influences editing efficiency. Second, in the cochlear samples collected from *in vivo* study for indel analysis, the hair cells only consist of a small portion of all the cochlear cells. Third, we identified large deletions from the samples of *in vivo* studies, which a standard indel analysis failed to detect. As we did not exhaustively characterize large deletions, our selective PCR based assay is likely to miss other deletions or DNA organizational changes.

Previous studies by us and others have shown that indel analysis using whole cochlea will substantially underestimate the editing efficiency primarily due to the scarcity of hair cells (13, 14). By single-cell whole genome amplification of purified hair cells for NGS, we detected a reduction in the allele frequency ratio from *Obl* to the WT after RNP delivery. While it is expected that in uninjected *Atp2b2*$^{Obl/+}$ inner ear, the allele frequency ratio of *Obl*:WT should be 50%:50%. The detected frequency ratio of *Obl*:WT, however, was 53%:47%, which was likely the result of the bias introduced during genome amplification that favored the *Obl* allele. After the injection, the *Obl* allele decreased by over 6% compared to untreated hair cells. If a similar biased genome amplification persists in the injected inner ear, 6% reduction in allele frequency in the *Atp2b2*$^{Obl/+}$ hair cells suggests a disruption on the *Obl* allele by editing in 25% of HCs, suggesting that as much as 25% of HC may regain the function of PMCA2 due to WT *Atp2b2* expression and thus the robust rescue of hearing. The lower *Obl* allele frequency after editing is consistent with the data that only the *Obl* allele was edited by RNP delivery of Cas9-*Atp2b2*-mut1 *in vitro* and *in vivo* (**Fig. 2a; Supplementary Fig. 2c**). Measuring the *Obl* vs WT allele frequency is also a better representation of

editing as larger deletions could be reflected by a shift in allele frequency but will be missed by indel analysis based on amplicons. Future improvement in unbiased genome amplification should facilitate the study of allele frequency in small number of cells, which in turn may offer a better assessment of editing efficiency that may be underestimated due to unconventional editing events including large deletions.

Liposomal mediated RNP delivery showed high-specificity and low off-target effect. In *in vitro* and *in vivo* samples with RNP delivery of *Atp2b2*-mut1, we only detected editing at the *Obl* locus. We assessed editing at off-target loci that could be modified by plasmid or RNP-based editing using computational prediction *(28)* and the GUIDE-seq method *(26)*. Among the top five software suggested off-targets, only one was shown to be edited at a low efficiency of 0.3% after plasmid nucleofection, whereas RNP delivery did not produce any indel. GUIDE-seq analysis revealed the only cleaved site was the *Atp2b2 sequence* after RNP delivery.

The *in vivo* rescue of OHC and auditory functions correlated with *in vitro* gRNA selection, i.e. the gRNA-mut1 with the highest allele specificity for the *Obl* locus produced the best outcome, whereas gRNA-mut2, despite its editing at the *Obl* locus (**Fig. 1c**), did not rescue either hearing or OHC function (**Supplementary Fig. 4a, b**). The study supports that a thorough *in vitro* selection of sgRNA could significantly impact *in vivo* result. The high specificity is demonstrated by the comparison of editing on the *Obl* and WT alleles. We showed that both *in vitro* and *in vivo* there is no editing on the WT allele and all editing is at the *Obl* allele.

While a majority of on-target editing consists of indels of less than 20 bp, recent studies have shown that the double strand breaks induced by CRISPR can also lead to large deletions, complex DNA rearrangements and chromosomal truncations in cell lines *(33, 34)* and zygotes *(35)*. Our results are in line with these studies and show for the first time that large deletions due to editing also occur *in vivo* in the inner ear after the administration of CRIPSR/Cas9 editing agents. Future development of CRISPR based therapy requires careful evaluation if such events lead to interruption of important exons or genes.

We further provide the evidence that the liposome RNP delivery system can be applied to improve hearing in mice carrying separate mutations in two genes. Genetic hearing loss due to digenic mutations is well documented *(18, 21–24)*. With the identification of increasing number of deafness genes, it is likely future intervention by editing therapy needs to target more than one mutation simultaneously. We took advantage of two dominant genetic hearing loss models, $Atp2b2^{Obl/+}$ and $Tmc1^{Bth/+}$ to create a double

mutant model (*Atp2b2*$^{Obl/+}$/*Tmc1*$^{Bth/+}$) with profound hearing loss at one month. It is significant that injection of Cas9 complexed with the double gRNAs of *Atp2b2*-mut1 and *Tmc1*-mut3 rescued hearing significantly whereas no hearing was rescued by a single gRNA delivery. The results suggest that in some hair cells both mutant *Obl* and *Bth* alleles have been edited that led to hearing recovery. This result is interesting given the fact that the delivery of each gRNA alone resulted in the editing efficiency of ~10% for Bth (Gao et al.2018) and 25% for *Obl*, thus a double editing of two mutations in the same hair cell is calculated around 2.5%. One possible explanation for hearing rescue in the double mutant mice is that the editing by the two gRNAs is not a random event, i.e. a hair cell may be preferentially edited by both gRNAs that gives rise to a skewed outcome. It is also possible that editing efficiency by each gRNA is higher than our data that was estimated to be the baseline for editing efficiency, which may contribute to higher number of hair cells being edited at both alleles. Another explanation is that editing in one hair cell may restore some function whereas collectively there is an additive effect when both gRNAs were delivered. Despite hearing in the two-gRNA injected double mutant inner ears is not rescued to the same level as each gRNA injected to *Atp2b2*$^{Obl/+}$ or *Tmc1*$^{Bth/+}$ individually, the moderate hearing improvement observed after liposomal mediated RNP delivery opens new avenues for further refinement of the approach as the treatment of diseases of multigenic origin.

Our work demonstrates the possibility of RNP delivery of editing agents into the inner ear to target out hair cell mutations and preserve hearing in the *Atp2b2*$^{Obl/+}$ mice. We have shown the RNP delivery is suitable for intervention of dominant mutations in all auditory hair cells. Combined with the evidence of the recue effect in the digenic mouse mutants with hearing loss, we have further widened the path for future development of editing base therapy for genetic hearing loss.

Methods

In vitro transcription of sgRNAs

Linear DNA fragments containing the T7 promoter binding site followed by the 20-bp sgRNA target sequence were obtained by PCR using Q5 High-Fidelity DNA Polymerase (NEB) with the primers listed in the supplementary information and 40ng of pFYF1320 (EGFP sgRNA expression plasmid) as a template according to the manufacturer's instructions. PCR products were purified using QUIAquick PCR purification kit (Qiagen) and transcribed in vitro using the T7 High Yield RNA Synthesis Kit (NEB) according to the manufacturer's instructions. sgRNA products were purified using the MEGAclear Transcription Clean-Up Kit (Ambion), quantified by Nanodrop and stored at -80°C.

In vitro DNA cleavage assay

Atp2b2$^{+/+}$ and *Atp2b2*$^{Obl/Obl}$ genomic DNA was isolated from mouse tail snips using the Agencourt DNAdvance Genomic DNA Isolation Kit (Beckman Coulter) according to the manufacturer's instructions. 956-bp *Atp2b2* DNA fragments were amplified from the genomic DNA and used as substrates for the *in vitro* cleavage reaction (Forward: GGACACTGAACCCCTGAGA; Reverse: GCCGAGAAAGGAGCTGACAT). Typically, the *Atp2b2* DNA fragment (150 nM) was incubated for 15 min at 37°C with 300 nM of purified Cas9 protein and sgRNA in Cas9 cleavage buffer (20 mM HEPES pH 7.5, 150 mM KCl, 0.5 mM DTT, 0.1 mM EDTA with10 mM MgCl2) in a total volume of 20 µL in each reaction. Reactions were quenched by adding 500 µL of PB wash buffer (Qiagen), purified on a QIAprep spin column and eluted in 20 µL 1X TE buffer. 10 µL of each reaction were loaded onto a 2% agarose gel and electrophoresed to separate starting DNA and cleaved products. Cas9-induced cleavage bands and the uncleaved band were visualized on an ChemiDoc MP and quantified using ImageJ software. The peak intensities of the cleaved bands were analyzed as previously described (36).

Construction of *Obl*-OC1 cell line

An *Atp2b2* gene fragment (2-kb) harboring the *Obl* mutation was amplified by PCR from *Atp2b2*$^{Obl/Obl}$ mouse genomic DNA using primers (Forward: CCCAAGCTTCGAGAGTTGGACTGAGGGTT; Reverse: ATAAGAATGCGGCCGCTAAGGGAGGTGGTGGAATCG). The PCR products were ligated into the restriction sites (HindIII and NotI) in the PiggyBac donor backbone (PB-CAG-mNeonGreen-P2A-BSD-polyA). The constructed donor plasmid was co-transfected with PiggyBac transposon vector (PB210PA, System Biosciences) in HEI-OC1 cells. Cells with inserted *Atp2b2* gene fragments carrying the *Obl* mutation were cultured and selected in the medium containing 10 µg/mL Blasticidin. Successful insertion was confirmed by PCR (Forward: GCCATGAACAAAGGTTGGCT; Reverse: GAGAGTCCAAACGAACCCCT) and sequencing analysis.

Delivery of protein complex or plasmids by nucleofection

Transfection programs were optimized following manufacturer's instruction (DS120, SG Cell Line 4D-Nucleofector^{TM} X Kit). 400 ng of pmaxGFP Control Vector (LONZA) was added to the nucleofection solution to assess nucleofection efficiencies in HEI-OC1, *Obl*-OC1 cells and primary fibroblasts. To deliver plasmids, cells were transfected using 1,000 ng Cas9 plasmid (pCas9), 500 ng sgRNA plasmid (pAtp2b2-mut1 sgRNA). To deliver protein complex, purified sgRNA was incubated with Cas9 protein for 5 min before transfection. Media was replaced ~16 h after nucleofection and cells were harvested for genomic DNA extraction after ~96 h.

General *in vivo* experiments

All in vivo experiments were carried out in accordance with NIH guidelines for the care and use of laboratory animals and were approved by the Massachusetts Eye & Ear Infirmary IACUC committee. Isogenic heterozygous *Obl/+* mice maintained on a C3HeB/FeJ (C3H) background were obtained from Wellcome Trust Sanger Institute. *Atp2b2*$^{Obl/+}$ mice were bred with *Tmc1Bth/Bth* to obtain *Pmca2*$^{Obl/+}$*Tmc1*$^{Bth/+}$ mice.

Microinjection into the inner ear of neonatal mice

A total of 112*Atp2b2*$^{Obl/+}$ mice (P0–2) of either sex were used for injections. The mice were randomly assigned to the different experimental groups, and at least three mice were injected in each group. Both surgical procedures and injections were performed as described previously (*13*). Briefly, 25 μM of Cas9 and sgRNA was mixed with Lipofectamine 2000 for 20 min at room temperature, and injected into the scala media of the cochlea at three different sites (base, middle and apex-middle turn). The volume for each injection was 0.3 μl with a total volume of 0.9 μl per cochlea. The release rate was 69 nl/min, controlled by a MICRO4 microinjection controller (WPI).

Acoustic testing

Auditory Brainstem Responses (ABR) and Distortion product otoacoustic emissions (DPOAE) were performed in a soundproof chamber as described previously (*13*). The acoustic tests were performed in mice up to 4 month-old anesthetized intraperitoneally with a mix of xylazine (10 mg/kg) and ketamine (100 mg/kg). Three subcutaneous needle electrodes placed at vertex, the ventral edge of the pinna and the tail (ground reference), were used for the recordings. Stimuli consisted in 5 ms tone pips (0.5 ms rise–fall with a cos2 onset, delivered at 35/s) presented at frequencies 16, 22.64, 32 and 45.25 kHz and delivered in 10 dB ascending steps from 20 to 90 dB (Sound Pressure Level, SPL). The response was amplified 10,000-fold, filtered (100 Hz–3 kHz passband), digitized, and averaged (1024 responses) at each SPL. Following visual inspection of stacked waveforms, ABR threshold was defined as the lowest SPL level at which any wave could be detected. Wave 1 amplitude was defined as the difference between the average of the 1-ms pre-stimulus baseline and the Wave 1 peak (P1). The cubic distortion product for DPOAE measurements was quantified in response to primaries f1 and f2. The primary tones were set as previously described (*13*). Threshold was computed by interpolation as the f2 level required to produce a DPOAE at 5 dB SPL.

Acoustic startle reflex

Mice were placed into a small, acoustically transparent cage resting atop a piezoelectric force plate in a sound attenuated booth. Acoustic stimuli and amplified force plate signals were encoded by a digital

signal processor (Tucker-Davis Technologies, RX6) using LabView scripts (National Instruments). Mice were placed in silence for 5 min to acclimate to the test environment before real measurements. A 16-kHz tone was presented at randomized intervals from an overhead speaker (50 dB to 120 dB SPL, 20 ms duration with 0 ms onset and offset ramps). Twelve repetitions were recorded for each of the intensities per test subject. Startle response amplitude was measured as the root mean square (RMS) voltage of the force plate signal shortly after sound presentation.

Immunohistochemistry and histology

Injected and non-injected cochleae were removed after animals were sacrificed by CO2 inhalation. Temporal bones were fixed in 4% paraformaldehyde at 4 °C overnight, and then decalcified in 120 mM EDTA for at least 1 week. When the bone was decalcified, the organ of Corti was dissected in pieces for whole-mount immunofluorescence. Nonspecific labeling was blocked with blocking solution (PBS with 8% donkey serum and 0.3 −1% Triton X-100) for 1 h at room temperature and followed by overnight incubation at room temperature with the primary antibody 1:300 mouse anti-Parvalbumin (Sigma P3088), 1:200 rabbit anti-pmca2 (PA1-915 ThermoFisher scientific). Tissues were incubated with the secondary antibody for 1h after three rinses with PBS. All Alexafluor secondary antibodies were from Invitrogen: donkey anti-rabbit Alex488 (A21206) and donkey anti- mouse Alex594 (A32744) was used as a 1:500 dilution. All specimens were mounted in ProLong Gold Antifade Mountant medium (P36930, Life Technologies). Confocal images were taken with a Leica TCS SP8 microscope using a 20X or 63X glycerin-immersion lens, with or without digital zoom. We acquired z-stacks by maximum intensity projections of z-stacks for each segment by imageJ (NIH image), and composite images showing the whole cochlea.

Hair cell isolation for DNA sequencing

Atp2b2$^{Olb/+}$ mice were injected with Cas9:Pmca2-mut1 sgRNA:Lipofectamine 2000 at P1 and were euthanized at P5. Cochleae were harvested with the sensory epithelia (GFP^+) dissociated using needles under the microscope (Axiovert 200M, Carl Zeiss), and immersed in 1 μM FM 1-43FX (PA1-915, ThermoFisher) dissolved in HBSS (ThermoFisher) for 30s at room temperature in the dark. The sensory epithelia were then transferred to 100 μl TrypleE Express Enzyme (12604013, ThermoFisher) with the GFP^+ cells isolated using a 1 μl pipette, Isolated hair cells were subjected to whole-genome amplification by MALBAC Single Cell WGA Kit (YK001A, Yikon Genomics) to isolate DNA for NGS analysis.

High-throughput DNA sequencing of genomic DNA samples

Treated cells or tissues were collected after four days and genomic DNA was isolated using the Agencourt DNAdvance Genomic DNA Isolation Kit (Beckman Coulter) according to the manufacturer's instructions. On-target and off-target genomic regions of interest were amplified by PCR with flanking primers (Forward: CCTCTCAAGGCTGTGCAGATGCT; Reverse: CCACGAAGAGCAGGGTGAAGATGA). PCR amplification was carried out with Q5 High-Fidelity DNA Polymerase (NEB) according to the manufacturer's instructions using 250 ng genomic DNA as a template. PCR products were purified using QUIAquick PCR purification kit (Qiagen). Samples were sequenced and analyzed to detect CRISPR variants from NGS reads using a custom algorithm developed by the Massachusetts General Hospital Center for Computational and Integrative Biology DNA Core. Individual SEQ files containing the variants were visualized by SnapGene.

GUIDE-seq analysis

To identify off-target sites, the GUIDE-seq method was performed essentially as previously described (GUIDE-seq ref) with the following modifications. Briefly, 100 nmole Cas9 (IDT, Cat # 1081059), 800 ng sgRNA (Synthego Co, Menlo Park, CA), and 1 pmol of the double-stranded oligodeoxynucleotide (dsODN) were nucleofected into *Obl*-OC1 cells. A sample nucleofected with dsODN only served as a negative control. Cells were harvested for genomic DNA extraction after 5 days and ~400ng of genomic DNA for each sample was sheared acoustically using a Covaris E220 sonicator to an average of 500 bp in 130 uL TE buffer. The GUIDE-seq sequencing libraries were prepared and sequenced on an Illumina Miseq as previously described *(26)*, with reads were mapped to the mouse reference genome (GRCm38). Off-target data analysis was initially performed with the standard pipeline, mapping the start position of the amplified sequences using a 10-bp sliding window, then retrieving the reference sequence around the site. Given the size of some of the deletions, the number of base pairs used as the flanking sequence was also increased to up to 10,000 bp. The retrieved sequences were aligned to the Cas9 target sequence using a Smith-Waterman local-alignment algorithm. The negative control sample treated with the dsODN but no Cas9 or sgRNA was used to assess background.

Statistical analysis

Statistical analyses were performed by two-way ANOVA with Bonferroni corrections for multiple comparisons for ABRs and DPOAEs, and by Student t-test for quantification of hair cell survival and hair cell transduction currents using the Prism 6.0 statistical analysis program (GraphPad).

Data availability

The authors declare that the relevant data supporting the findings of this study are available within the paper and its supplementary information files

References

1. L. Z. X. Angeli S, Lin X, Genetic of Hearing and defness. *Anat Rec*. **40**, 1291–1296 (2015).

2. G. S. G. Géléoc, J. R. Holt, Sound strategies for hearing restoration. *Science (80-.).* **344** (2014), doi:10.1126/science.1241062.

3. U. Müller, P. G. Barr-Gillespie, New treatment options for hearing loss. *Nat. Rev. Drug Discov.* **14**, 346–365 (2015).

4. C. Askew, C. Rochat, B. Pan, Y. Asai, H. Ahmed, E. Child, B. L. Schneider, P. Aebischer, J. R. Holt, Tmc gene therapy restores auditory function in deaf mice. *Sci. Transl. Med.* **7**, 1–12 (2015).

5. C. A. Nist-Lund, B. Pan, A. Patterson, Y. Asai, T. Chen, W. Zhou, H. Zhu, S. Romero, J. Resnik, D. B. Polley, G. S. Géléoc, J. R. Holt, Improved TMC1 gene therapy restores hearing and balance in mice with genetic inner ear disorders. *Nat. Commun.* **10**, 1–14 (2019).

6. A. Ponnath, F. F. Depreux, F. M. Jodelka, F. Rigo, H. E. Farris, M. L. Hastings, J. J. Lentz, Rescue of Outer Hair Cells with Antisense Oligonucleotides in Usher Mice Is Dependent on Age of Treatment. *JARO - J. Assoc. Res. Otolaryngol.* **19**, 1–16 (2018).

7. S. B. Shibata, P. T. Ranum, H. Moteki, B. Pan, A. T. Goodwin, S. S. Goodman, P. J. Abbas, J. R. Holt, R. J. H. Smith, RNA Interference Prevents Autosomal-Dominant Hearing Loss. *Am. J. Hum. Genet.* **98**, 1101–1113 (2016).

8. J. A. Zuris, D. B. Thompson, Y. Shu, J. P. Guilinger, J. L. Bessen, J. H. Hu, M. L. Maeder, J. K. Joung, Z. Y. Chen, D. R. Liu, Cationic lipid-mediated delivery of proteins enables efficient protein-based genome editing in vitro and in vivo. *Nat. Biotechnol.* **33**, 73–80 (2015).

9. H. Yin, C. Q. Song, J. R. Dorkin, L. J. Zhu, Y. Li, Q. Wu, A. Park, J. Yang, S. Suresh, A. Bizhanova, A. Gupta, M. F. Bolukbasi, S. Walsh, R. L. Bogorad, G. Gao, Z. Weng, Y. Dong, V. Koteliansky, S. A. Wolfe, R. Langer, W. Xue, D. G. Anderson, Therapeutic genome editing by combined viral and non-viral delivery of CRISPR system components in vivo. *Nat. Biotechnol.* **34**, 328–333 (2016).

10. Y. Yang, L. Wang, P. Bell, D. McMenamin, Z. He, J. White, H. Yu, C. Xu, H. Morizono, K. Musunuru, M. L. Batshaw, J. M. Wilson, A dual AAV system enables the Cas9-mediated correction of a metabolic liver disease in newborn mice. *Nat. Biotechnol.* **34**, 334–338 (2016).

11. C. Long, C. Long, L. Amoasii, A. A. Mireault, J. R. Mcanally, H. Li, E. Sanchez-, S. Bhattacharyya, J. M. Shelton, R. Bassel-duby, E. N. Olson, Science-2015-Long-science.aad5725. **5725** (2015).

12. S. Kim, D. Kim, S. W. Cho, J. Kim, J. S. Kim, Highly efficient RNA-guided genome editing in human cells via delivery of purified Cas9 ribonucleoproteins. *Genome Res.* **24**, 1012–1019 (2014).

13. X. Gao, Y. Tao, V. Lamas, M. Huang, W. Yeh, B. Pan, Y. Hu, J. H. Hu, D. B. Thompson, Y. Shu, H. Wang, S. Yang, Q. Xu, D. B. Polley, M. Charles, W. Kong, J. R. Holt, Z. Chen, D. R. Liu, Treatment of autosomal dominant hearing loss by in vivo delivery of genome editing agents. **553**, 217–221 (2018).

14. B. György, C. Nist-Lund, B. Pan, Y. Asai, K. D. Karavitaki, B. P. Kleinstiver, S. P. Garcia, M. P. Zaborowski, P. Solanes, S. Spataro, B. L. Schneider, J. K. Joung, G. S. G. Géléoc, J. R. Holt, D. P. Corey, Allele-specific gene editing prevents deafness in a model of dominant progressive hearing loss. *Nat. Med.* **25**, 1123–1130 (2019).

15. W. H. Yeh, O. Shubina-Oleinik, J. M. Levy, B. Pan, G. A. Newby, M. Wornow, R. Burt, J. C. Chen, J. R. Holt, D. R. Liu, In vivo base editing restores sensory transduction and transiently improves auditory function in a mouse model of recessive deafness. *Sci. Transl. Med.* **12** (2020), doi:10.1126/scitranslmed.aay9101.

16. C. C. Morton, W. E. Nance, Newborn Hearing Screening — A Silent Revolution. *N. Engl. J. Med.* **354**, 2151–2164 (2006).

17. R. A. Dumont, U. Lins, A. G. Filoteo, J. T. Penniston, B. Kachar, P. G. Gillespie, Plasma membrane Ca2+-ATPase isoform 2a is the PMCA of hair bundles. *J. Neurosci.* **21**, 5066–78 (2001).

18. J. M. Schultz, Y. Yang, A. J. Caride, A. G. Filoteo, A. R. Penheiter, A. Lagziel, R. J. Morell, S. A. Mohiddin, L. Fananapazir, A. C. Madeo, J. T. Penniston, A. J. Griffith, Modification of Human Hearing Loss by Plasma-Membrane Calcium Pump PMCA2. *N. Engl. J. Med.* **352**, 1557–1564 (2005).

19. J. J. Smits, J. Oostrik, A. J. Beynon, S. G. Kant, P. A. M. de Koning Gans, L. J. C. Rotteveel, J. S. Klein Wassink-Ruiter, R. H. Free, S. M. Maas, J. van de Kamp, P. Merkus, W. Koole, I. Feenstra, R. J. C. Admiraal, C. P. Lanting, M. Schraders, H. G. Yntema, R. J. E. Pennings, H. Kremer, De novo and inherited loss-of-function variants of ATP2B2 are associated with rapidly progressive hearing impairment. *Hum. Genet.* **138**, 61–72 (2019).

20. S. L. Spiden, M. Bortolozzi, F. Di Leva, M. H. de Angelis, H. Fuchs, D. Lim, S. Ortolano, N. J. Ingham, M. Brini, E. Carafoli, F. Mammano, K. P. Steel, The novel mouse mutation Oblivion inactivates the PMCA2 pump and causes progressive hearing loss. *PLoS Genet.* **4**, e1000238 (2008).

21. A. Pandya, K. S. Arnos, X. J. Xia, K. O. Welch, S. H. Blanton, T. B. Friedman, G. Garcia Sanchez, X. Z. Liu, R. Morell, W. E. Nance, Frequency and distribution of GJB2 (connexin 26) and GJBG (connexin 30) mutations in a large North American repository of deaf probands. *Genet. Med.* **5**, 295–303 (2003).

22. X. Z. Liu, Y. Yuan, D. Yan, E. H. Ding, X. M. Ouyang, Y. Fei, W. Tang, H. Yuan, Q. Chang, L. L. Du, X. Zhang, G. Wang, S. Ahmad, D. Y. Kang, X. Lin, P. Dai, Digenic inheritance of non-syndromic deafness

caused by mutations at the gap junction proteins Cx26 and Cx31. *Hum. Genet.* **125**, 53–62 (2009).

23. M. Li, S. ya Nishio, C. Naruse, M. Riddell, S. Sapski, T. Katsuno, T. Hikita, F. Mizapourshafiyi, F. M. Smith, L. T. Cooper, M. G. Lee, M. Asano, T. Boettger, M. Krueger, A. Wietelmann, J. Graumann, B. W. Day, A. W. Boyd, S. Offermanns, S. ichiro Kitajiri, S. ichi Usami, M. Nakayama, Digenic inheritance of mutations in EPHA2 and SLC26A4 in Pendred syndrome. *Nat. Commun.* **11** (2020), doi:10.1038/s41467-020-15198-9.

24. Q. Y. Zheng, D. Yan, X. M. Ouyang, L. L. Du, H. Yu, B. Chang, K. R. Johnson, X. Z. Liu, B. Harbor, Digenic inheritance of deafness caused by mutations in genes encoding cadherin 23 and protocadherin 15 in mice and humans. **14**, 103–111 (2010).

25. F. Kalinec, G. Kalinec, M. Boukhvalova, B. Kachar, Cell Biology International 1999 KALINEC. **23**, 175–184 (1999).

26. S. Q. Tsai, Z. Zheng, N. T. Nguyen, M. Liebers, V. Ved, V. Thapar, N. Wyvekens, C. Khayter, A. J. Iafrate, P. Le, M. J. Aryee, J. K. Joung, P. Unit, M. G. Hospital, M. G. Hospital, K. Institutet, GUIDE-Seq enables genome-wide profiling of off-target cleavage by CRISPR-Cas nucleases. **33**, 187–197 (2015).

27. A. C. Komor, A. H. Badran, D. R. Liu, CRISPR-Based Technologies for the Manipulation of Eukaryotic Genomes. *Cell*. **169**, 559 (2017).

28. F. Zhang, CRISPR DESIGN. *http://crispr.mit.edu* (2015).

29. T. Calì, M. Brini, E. Carafoli, Regulation of Cell Calcium and Role of Plasma Membrane Calcium ATPases. *Int. Rev. Cell Mol. Biol.* **332**, 259–296 (2017).

30. P. Dai, L. H. Huang, G. J. Wang, X. Gao, C. Y. Qu, X. W. Chen, F. R. Ma, J. Zhang, W. L. Xing, S. Y. Xi, B. R. Ma, Y. Pan, X. H. Cheng, H. Duan, Y. Y. Yuan, L. P. Zhao, L. Chang, R. Z. Gao, H. H. Liu, W. Zhang, S. S. Huang, D. Y. Kang, W. Liang, K. Zhang, H. Jiang, Y. L. Guo, Y. Zhou, W. X. Zhang, F. Lyu, Y. N. Jin, Z. Zhou, H. L. Lu, X. Zhang, P. Liu, J. Ke, J. S. Hao, H. M. Huang, D. Jiang, X. Ni, M. Long, L. Zhang, J. Qiao, C. C. Morton, X. Z. Liu, J. Cheng, D. M. Han, Concurrent Hearing and Genetic Screening of 180,469 Neonates with Follow-up in Beijing, China. *Am. J. Hum. Genet.* **105**, 803–812 (2019).

31. D. Kooshavar, M. A. Tabatabaiefar, E. Farrokhi, M. Abolhasani, M. R. Noori-Daloii, M. Hashemzadeh-Chaleshtori, Digenic inheritance in autosomal recessive non-syndromic hearing loss cases carrying GJB2 heterozygote mutations: Assessment of GJB4, GJA1, and GJC3. *Int. J. Pediatr. Otorhinolaryngol.* **77**, 189–193 (2013).

32. I. J. Russell, Cochlear Receptor Potentials. *Senses A Compr. Ref.* **3**, 319–358 (2008).

33. G. Cullot, J. Boutin, J. Toutain, F. Prat, P. Pennamen, C. Rooryck, M. Teichmann, E. Rousseau, I. Lamrissi-Garcia, V. Guyonnet-Duperat, A. Bibeyran, M. Lalanne, V. Prouzet-Mauléon, B. Turcq, C. Ged, J. M.

Blouin, E. Richard, S. Dabernat, F. Moreau-Gaudry, A. Bedel, CRISPR-Cas9 genome editing induces megabase-scale chromosomal truncations. *Nat. Commun.* **10**, 1–14 (2019).

34. M. Kosicki, K. Tomberg, A. Bradley, Repair of double-strand breaks induced by CRISPR–Cas9 leads to large deletions and complex rearrangements. *Nat. Biotechnol.* **36**, 765–771 (2018).

35. A. Korablev, V. Lukyanchikova, I. Serova, N. Battulin, On-target CRISPR/CAS9 activity can cause undesigned large deletion in mouse zygotes. *Int. J. Mol. Sci.* **21**, 16–18 (2020).

Declarations

Funding: This work was supported by U.S. NIH R01 DC016875, UG3TR002636, U24HG010423, Curing Kids Massachusetts Eye & Ear and Ines-Fredrick Yeatts Fund (to Z-Y.C.), and Margaret Q. Landenberger Research Foundation (to B.P.K). Also, by U.S. NIH UG3AI150551, U01AI142756, R35GM118062, RM1HG009490, and HHMI (to D.R.L).

Author contributions:

Conceptualization: YT, VL, JZ, DT, DRL, ZYC

Methodology: YT, VL, YL, WD, MNW, WZ, JZ, DT, YS, XG, JH, BPK, DRL, ZYC

Experiment: VL, YT, YL, WD, MNW, WZ, JZ, DT, YS, XG, JH

Data analysis: all authors

Supervision: DRL, ZYC

Manuscript writing: VL, YL, YT, ZYC

Manuscript review and editing: All authors

Competing interests: Z-Y.C is a cofounder of Salubritas Therapeutics and scientific advisor to Rescue Hearing Inc. He and D.R.L have filed patent applications on: Efficient delivery of therapeutic molecules in vitro and in vivo" (**15/523325**) and "Method for efficient delivery of therapeutic molecules in vitro and in vivo" (**15/523321**)**.** B.P.K is an inventor on patents and patent applications filed by Mass General Brigham that describe genome engineering technologies. B.P.K. is a consultant for Avectas Inc., EcoR1 capital, and ElevateBio, and is an advisor to Acrigen Biosciences and Life Edit Therapeutics.

Figures

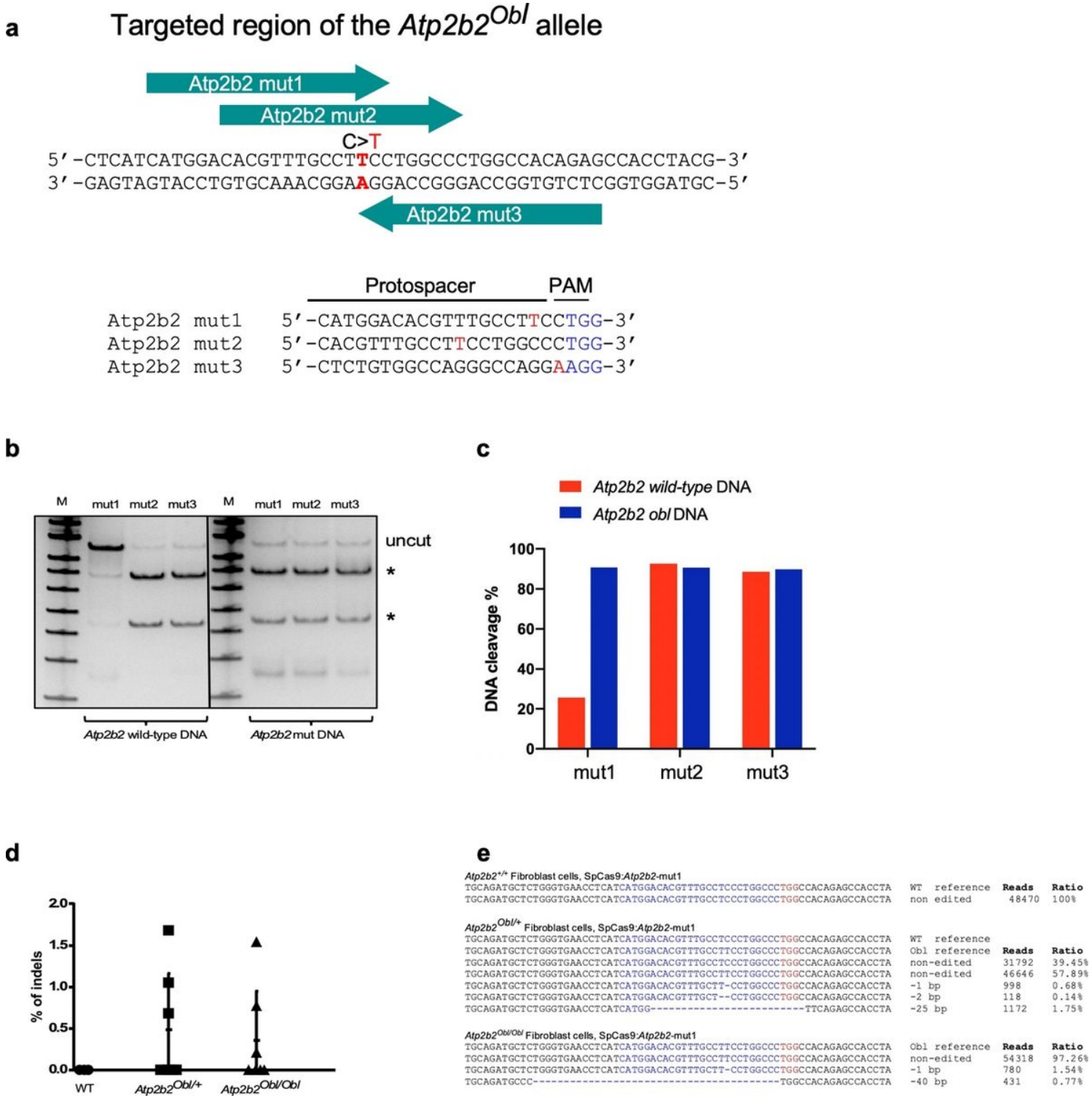

Figure 1

Design of a genome-editing strategy to disrupt the *Obl* mutant allele. (a) SpCas9 sgRNAs were designed to target the mutant *Atp2b2 Obl* allele, in which C2765 is changed to T (red). The protospacer (green arrows) of each *Obl*-targeting sgRNA contains a complementary A or T (red) that pairs with the mutation in the *Obl* allele, but that forms a mismatch with wildtype *Atp2b2* allele. (**b)** *In vitro* Cas9:sgRNA-mediated *Atp2b2* DNA cleavage. 50 nM of a 956-bp DNA fragments of *Atp2b2* or the *Atp2b2*$^{Obl/+}$ was incubated with 300 nM of each of the three Cas9:sgRNA for 15 min at 37ºC. Expected cleavage products of 553-bp

and 403-bp were detected in all samples as shown by asterisks. M=100bp ladder. (**c)** Quantification of DNA cleavage in **b** by densitometry using imageJ. (**d)** Editing shown by the indel percentages in three unsorted adult mouse primary fibroblast cells (WT, *Atp2b2*$^{Obl/+}$ *and Atp2b2*$^{Obl/Obl}$) after nucleofection of the RNP complex of Cas9:*Atp2b2*-mut1 gRNA. Indels were detected in the cells with the Obl allele. (**e**) NGS reads of indel from D. The *Obl* mutation was boxed (green). The list of indels is not comprehensive, only the top representative indels were shown.

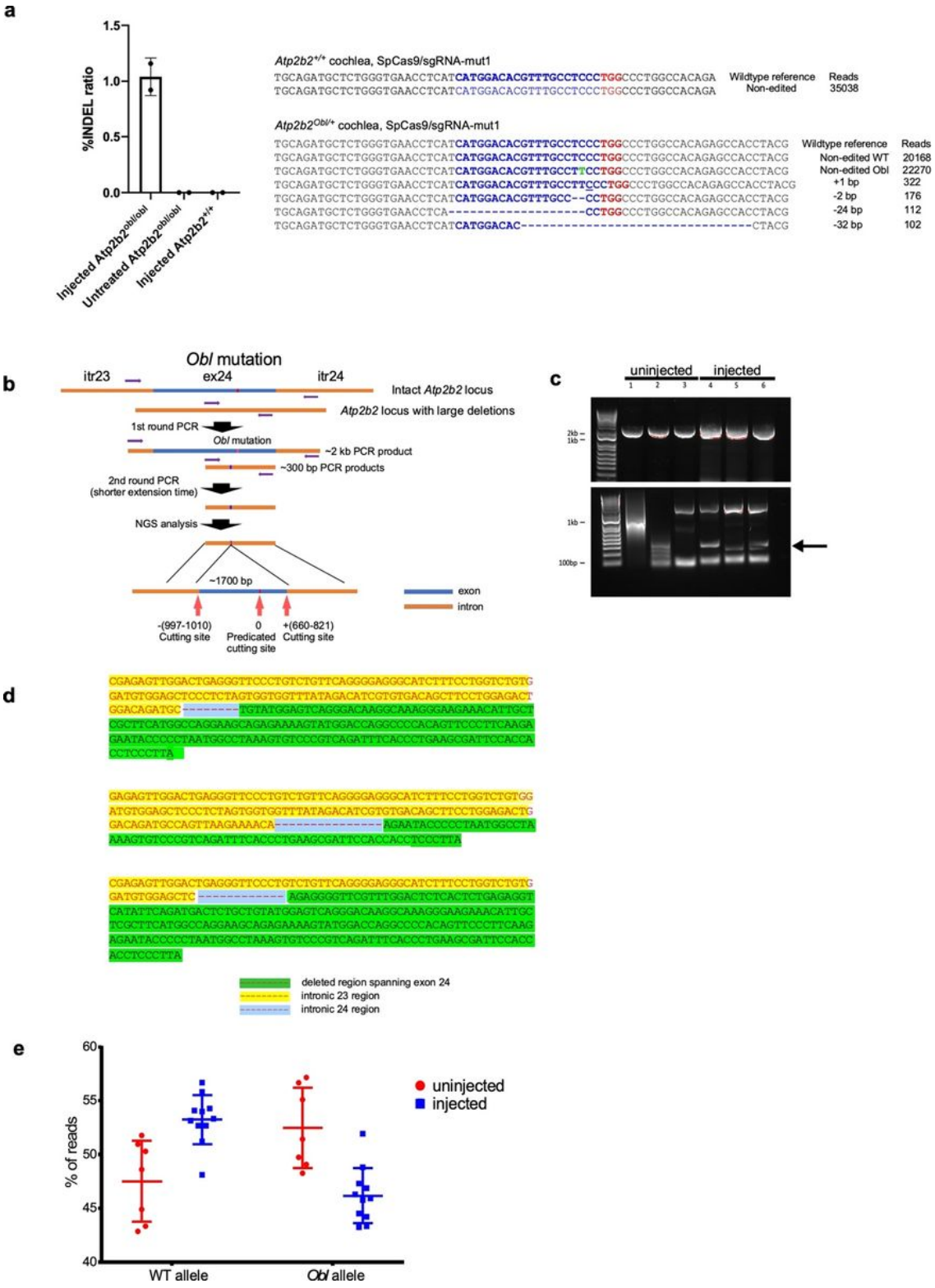

Figure 2

***In vivo* gene editing by RNP injection in *Atp2b2 Obl* mutant mice. (a)** Indel frequencies on the *Obl* allele from injected *Atp2b2*$^{obl/+}$ or *Atp2b2*$^{+/+}$ organ of Corti samples 4 days after injection of Cas9-GFP:*Atp2b2*-mut1:Lipo2000 or from uninjected *Atp2b2*$^{obl/+}$organ of Corti. The most abundant editing events by small deletions at the *Atp2b2* sequences, grouped by similarity, from organ of Corti samples are shown on the right. The PMA sites were marked red. The *Obl* mutation is highlighted in green. (**b)** A schematic representation of nested PCR to detect large deletions resulted from injection of Cas9-GFP:*Atp2b2*-mut1:Lipo2000. Itr: intron; ex: exon. (**c)** Gel image of the nested PCR products. Upper panel shows the 2kb fragments obtained from the 1st round PCR, which were used as the template for the 2nd round of PCR. Bottom panel shows the small fragments of varying sizes (arrow) obtained after PCR with the nested primers and a shorter extension time. (**d)** Sanger sequencing of smaller nested PCR products showed deletions that spanned the entire exon 24 with the *Obl* mutation. Each deletion had different genomic ends, an implication of variable cutting sites by Cas9. (**e)** Comparison of WT and *Obl* allele frequency from purified *Atp2b2*$^{ob/+}$ hair cells showed a shift that increased the WT allele frequency and decreased the *Obl* allele frequency after *in vivo* injection of the Lipo:Cas9:*Atp2b2*-mut1 RNP complex compared to uninjected *Atp2b2*$^{obl/+}$ hair cells. The dots represented independently purified hair cell groups from five animals.

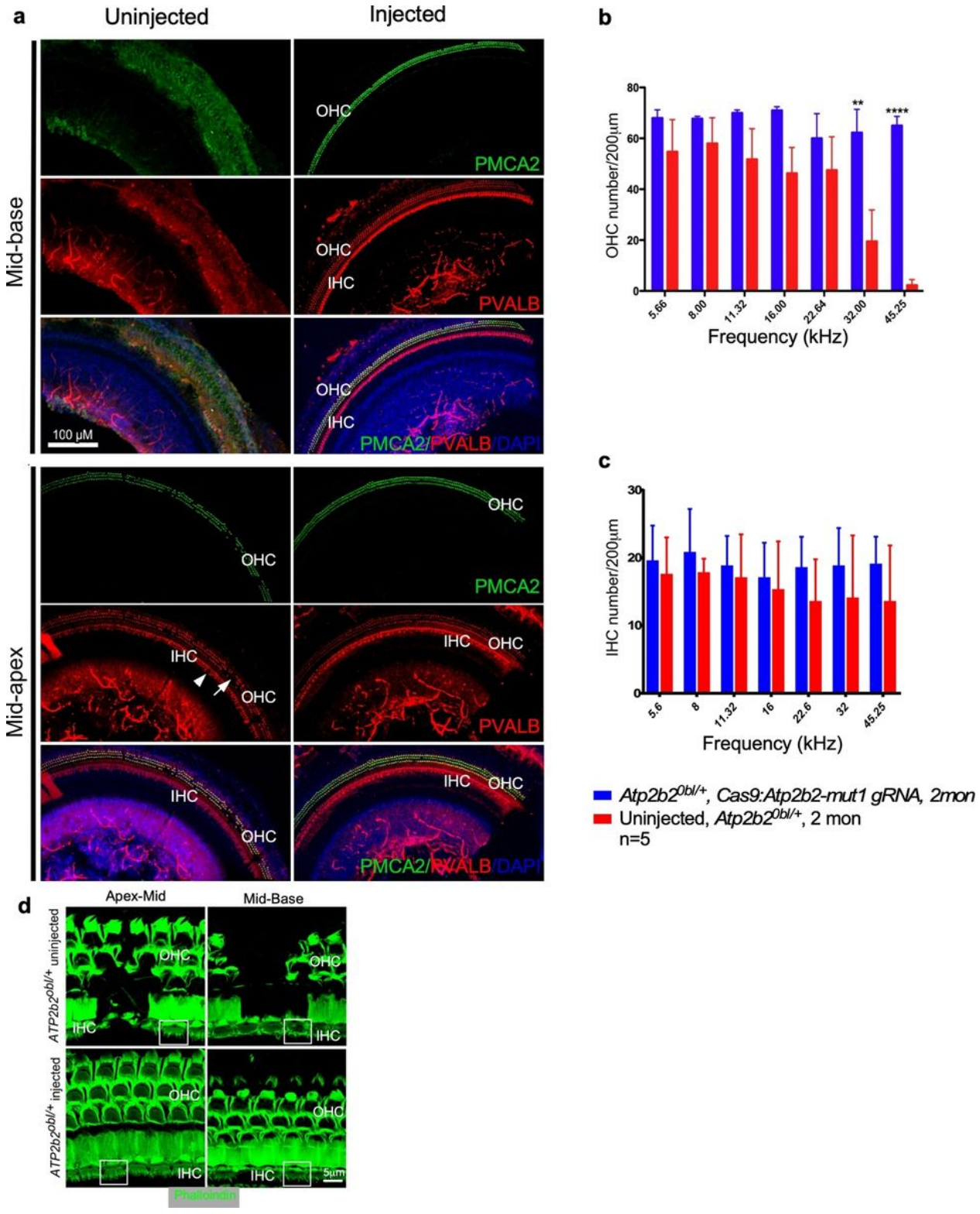

Figure 3

***In vivo* lipid mediated RNP delivery of Cas9:sgRNA complexes improves hair cell survival. (a)** Representative confocal microscopy whole mount images from uninjected *Atp2b2*$^{Obl/+}$ cochlea (left) and cochlea injected with Cas9:*Atp2b2*-mut1 sgRNA:Lipo2000 complex (right) at P1 with the cochleae harvested at two months of age. PMCA2 labeled OHC (PMCA2/PVALB) was detected in the injected *Atp2b2*$^{Obl/+}$ cochlea and was missing in the uninjected contralateral control cochlea in the mid-base turn.

In the mid-apical turn, OHCs were seen in injected and uninjected *Atp2b2*$^{Obl/+}$ cochleae. (**b & c)** Quantification of OHC **(b)** and IHC **(c)** survival in *Atp2b2*$^{Obl/+}$ mice 8 weeks after Cas9:*Atp2b2*-mut1 sgRNA:Lipo2000 injection (blue) compared to uninjected (red) contralateral ears across frequency regions. Values and error bars reflect the mean ± SEM of five mice (n=5). Statistical tests were two-way ANOVA with Bonferroni correction for multiple comparisons: **p < 0.01 and ****p < 0.0001. (**d)** Phalloidin labelling showed the preservation of hair cell stereocilia in a cochlea eight weeks after injection with Cas9:*Atp2b2*-mut1 sgRNA at two frequency regions, whereas the uninjected contralateral inner ear of the same mouse showed the loss of hair cells and severe degeneration of stereocilia at the same frequency regions. The boxes indicate the stereocilia. In the apex-mid region, a normal distribution of inner hair cell (IHC) stereocilia was seen in an injected ear, contrasting to fewer stereocilia in IHC in the contralateral uninjected ear. In the mid-base region, the stereocilia were no longer visible in the uninjected IHC compared to stereocilia in the contralateral injected IHC.

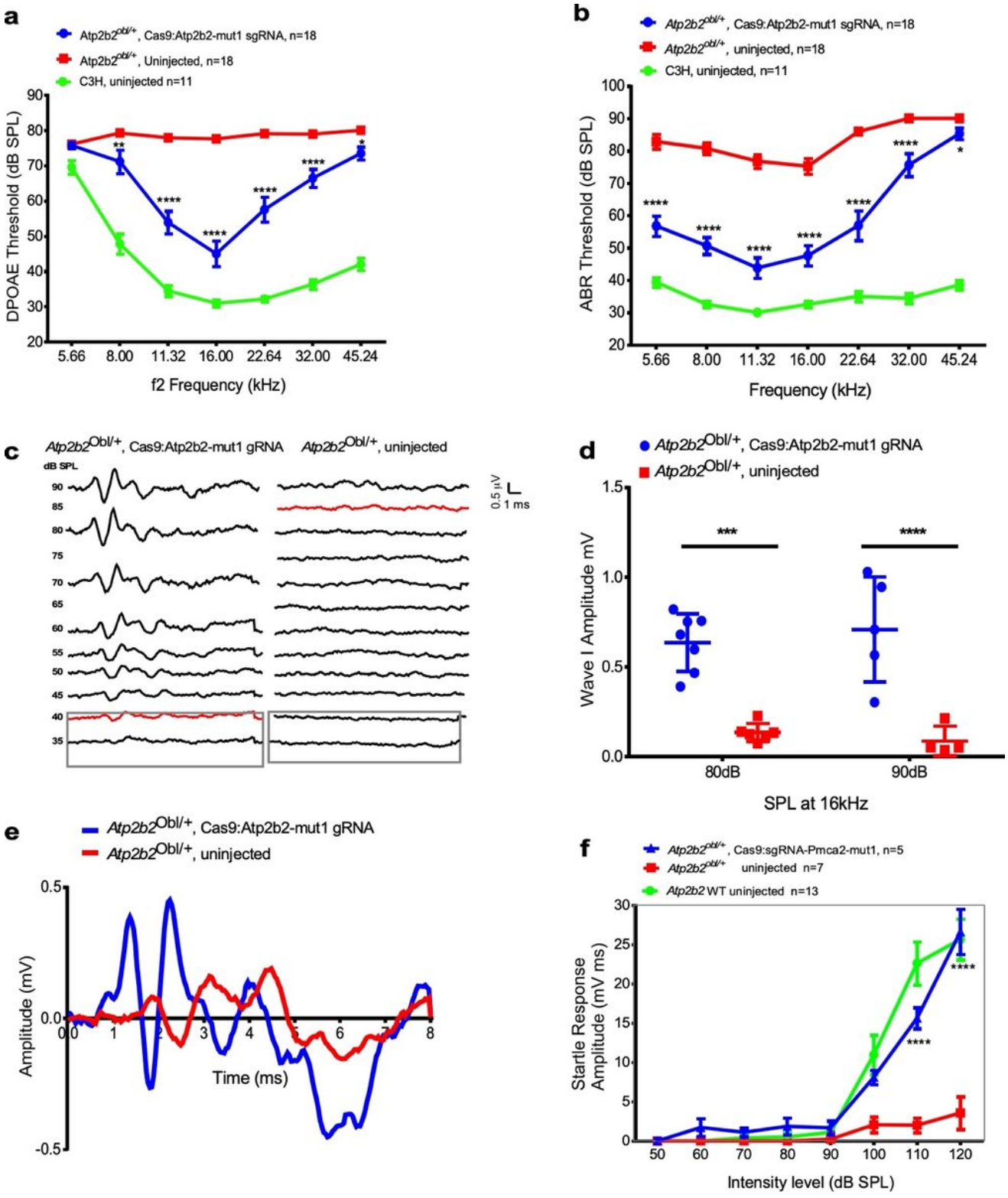

Figure 4

***In vivo* lipid mediated delivery of Cas9:sgRNA complexes rescues OHC function, hearing and auditory behavioral function. a.** DPOAE thresholds in *Atp2b2*$^{Obl/+}$ ears injected with Cas9:*Atp2b2*-mut1 sgRNA:Lipo2000 (blue), uninjected *Atp2b2*$^{Obl/+}$ ears (red), and wildtype C3H ears (green) after 4 weeks. **b.** ABR thresholds in *Atp2b2*$^{Obl/+}$ ears injected with Cas9:*Atp2b2*-mut1 sgRNA:Lipo2000 (blue), uninjected

Atp2b2$^{Obl/+}$ ears (red), and wildtype C3H ears (green) after 4 weeks. **c.** Representative ABR waveforms illustrating reduced threshold of 40 dB (red trace, left) at 16 kHz in a Cas9:*Atp2b2*-mut1 gRNA injected *Atp2b2*$^{Obl/+}$ inner ear compared to threshold of 85 dB (red trace, right) of the uninjected contralateral ear of the same mouse four weeks after injection. **d**. Amplitudes of ABR Wave 1 at 16 kHz in Cas9:*Atp2b2*-mut1 sgRNA:Lipo2000-injected ears (blue) compared with uninjected ears (red) after 4 weeks. **e.** Mean ABR waveforms at 16kHz in Cas9:*Atp2b2*-mut1 sgRNA:Lipo2000- *Atp2b2*$^{Obl/+}$ injected ears (blue) and uninjected ears (red). **f.** Startle responses in Cas9:*Atp2b2*-mut1 sgRNA:Lipo2000 injected mice (blue), uninjected mice (red) and wildtypeC3H ears (green) at 8 weeks post injection. Statistical tests were two-way ANOVA with Bonferroni correction for multiple comparisons: **p < 0.01, ***p < 0.001, and ****p < 0.0001. Values and error bars are mean ± SEM.

Supplementary Files

This is a list of supplementary files associated with this preprint. Click to download.

- pmca2supplementaryinformationv1.docx
- a2rs.pdf